Identification of Trapped and Boundary Lipid Binding Sites in M13 Coat Protein/Lipid Complexes by Deuterium NMR Spectroscopy†

L. C. M. Van Gorkom,‡ L. I. Horváth,§ M. A. Hemminga,∥ B. Sternberg,⊥ and A. Watts*,‡

Department of Biochemistry, University of Oxford, South Parks Road, Oxford OX1 3QU, United Kingdom, Institute of Biophysics, Biological Research Centre of Hungarian Academy of Sciences, P.O. Box 521, Szeged H-6701, Hungary, Department of Molecular Physics, Agricultural University, Dreijenlaan 3, 6703 HA Wageningen, The Netherlands, and Department of Electron Microscopy, Friedrich-Schiller University Jena, Ziegelmühlenweg 1, 6900 Jena, GDR

Received August 31, 1989; Revised Manuscript Received November 27, 1989

ABSTRACT: The major coat protein of M13 bacteriophage has been incorporated into bilayers of 1,2-dimyristoyl-*sn*-glycero-3-phosphocholine, deuterated in the trimethyl segments of the choline headgroup (DMPC-d_9). Two-component deuterium and phosphorus-31 NMR spectra have been observed from bilayer complexes containing the coat protein, indicating slow exchange (on the deuterium quadrupole anisotropy and phosphorus-31 chemical shift averaging time scales) of lipid molecules of $<10^3$ Hz between two motionally distinct environments in the complexes. The fraction of the isotropic spectral component increases with increasing M13 protein concentration, and this component is attributed to lipid headgroups, which are disordered relative to their order in protein-free bilayers. The activation energy of the fast local motions of the trimethyl groups of the choline residue in the headgroup decreases from 23 kJ mol^{-1} in the pure lipid bilayers to 20 kJ mol^{-1} for the protein-associated lipid headgroups. The chemical exchange rate of lipid molecules between the two motionally distinct environments has been estimated to be 20–50 Hz by steady-state line-shape simulations of the deuterium spectra of DMPC-d_9/M13 coat protein complexes using exchange-coupled modified Bloch equations. The off-rate was, as expected from one-to-one exchange, independent of the L/P ratio; τ_{off}^{-1} = 0.23 kHz. It is suggested that the protein-associated lipid may be trapped between closely packed parallel aggregates of M13 coat protein and that the high local concentration of protein in a one-dimensional arrangement in lipid bilayers may be required for the fast reassembly of phage particles before release from an infected cell.

The bacteriophage M13 consists of a circular single-stranded DNA molecule covered by a coat protein (MW = 5240) (Chamberlain et al., 1978; Beck et al., 1978; Van Wezenbeek et al., 1980). The bacteriophage M13 enters the *Escherichia coli* cell via a sex pilus, and during the infection period parental and newly synthesized coat protein are stored as an integral protein in the cytoplasmic cell membrane (Marvin & Wachtel, 1975; Wickner, 1976). The virus particle assembly is membrane associated. A pro-coat protein is produced by the infected host cell which is converted into the mature coat protein by a leader peptidase (Kuhn et al., 1986). After reassembly the new bacteriophage M13 leaves the cell without lysis of the host cell. The coat protein undergoes a significant conformational change in the disassembly and reassembly processes of the phage particles (Nozaki et al., 1976). The secondary structure in the intact virus particle is 100% α-helical, although during storage in the cell membrane it has a predominantly β-sheet structure (Marvin et al., 1974, 1975). M13 coat protein is an amphomorphic membrane protein whose secondary structure within the membrane depends on the L/P ratio[1] as well as the chemical nature of the lipid acyl chain and the polar headgroups (Chamberlain et al., 1978; Fodor et al., 1981; Makino et al., 1975; Cavalieri et al., 1976; Spruijt et al., 1989).

High-resolution multinuclear NMR spectroscopy has been performed on dimers of coat protein of bacteriophage M13 and related phages (f1 and fd) in SDS micelles and sonicated phospholipid vesicles. This gives detailed information about secondary structure and mobility of M13 coat protein dimers (Cross & Opella, 1980; Henry et al., 1986a,b; Leo et al., 1987; Bogusky et al., 1987). Deuterium NMR spectroscopy, using chain-deuterated palmitic acid, shows motional restriction of the palmitic acyl chains by the M13 coat protein in DMPC/palmitic acid/M13 coat protein complexes (Datema et al., 1988a). Deuterium NMR spectroscopy of amino-deuterated M13 coat protein in bilayers indicates that the protein is aggregated (Datema et al., 1988b), which is supported by fluorescence spectroscopy (Datema et al., 1987a). ESR experiments of DMPC/M13 coat protein complexes (Datema et al., 1987b) show a greater affinity of the M13 coat protein for negatively charged phospholipids.

In this work, the perturbation of the membrane surface by the coat protein has been investigated, as in other systems (Watts, 1987), by deuterium NMR methods. M13 coat protein has been incorporated at a range of lipid/protein ratios, into bilayers of DMPC deuterated in the trimethyl segments

† This work was supported by the Commission of the European Communities (ST-2J-0088 to A.W. and M.A.H.) and SERC (GR/D/22889 and GR/D/02218 to A.W.).

* Author to whom correspondence should be addressed.
‡ University of Oxford.
§ Biological Research Centre of Hungarian Academy of Sciences.
∥ Agricultural University.
⊥ Friedrich-Schiller University Jena.

[1] Abbreviations: ESR, electron spin resonance; NMR, nuclear magnetic resonance; CD, circular dichroism; HPLC, high-performance liquid chromatography; TLC, thin-layer chromatography; SDS, sodium dodecyl sulfate; EDTA, ethylenediaminetetraacetic acid; Tris-HCl, tris(hydroxymethyl)aminomethane hydrochloride; L/P ratio, DMPC-d_9 to M13 coat protein molar ratio; DMPC, 1,2-dimyristoyl-*sn*-glycero-3-phosphocholine; DMPE, 1,2-dimyristoyl-*sn*-glycero-3-phosphoethanolamine; 14-PCSL, 1-acyl-2-[13-(2-butyl-4,4-dimethyl-3-oxy-2-oxazolidinyl)tridecanoyl]-*sn*-glycero-3-phosphocholine; CSA, chemical shift anisotropy.

0006-2960/90/0429-3828$02.50/0

of the choline headgroup at a range of L/P ratios, and the perturbation of the labeled lipid segments studied.

Materials and Methods

Phospholipid Synthesis. The phospholipid, 1,2-dimyristoyl-*sn*-glycero-3-phosphocholine (DMPC), was specifically deuterated in the trimethyl groups of the choline moiety by methylation of DMPE with deuterated methyl iodide, as described by Eibl (1980). This DMPC-d_9 was purified by HPLC on a LiChroprep Si 60 column that was eluted with a chlorform/methanol/ammonia solvent system of successively increasing polarity and then by crystallization from acetone at −20 °C. After purification, the lipid appeared as one spot on high-performance silica TLC (solvent: $CHCl_3$/MeOH/NH_4OH, 65:30:3) and was stored at −20 °C until required.

Protein Purification. Bacteriophage M13 was grown and isolated as described earlier (Garsen et al., 1977). The major coat protein was isolated from the phage according to Knippers and Hoffmann-Berling (1966).

Protein Reconstitution (Datema et al., 1988a). Required amounts of DMPC-d_9 together with M13 coat protein were dissolved in 8.0 M urea/5.0 mM Tris-HCl/0.1 mM EDTA/20 mM ammonium sulfate/2% (w/w) sodium cholate buffer (pH 8.0) by vortexing and heating to 55 °C until a clear solution was obtained. Solubilization was monitored visually, and no precipitate of unincorporated water-insoluble coat protein was observed. After solubilization, the suspension was dialyzed at 25 °C against a 100-fold excess of 10 mM Tris-HCl/0.2 mM EDTA/10% (v/v) methanol buffer (pH 8.0) for a total of 120 h with changes at 24, 48, 72, and 96 h. In the last two steps methanol was omitted from the dialysis buffer. After dialysis the residual solvent was removed by freeze-drying. The solid mixture of lipid and M13 coat protein was resuspended in deuterium-depleted water at a ratio of 1:2 (w/w). The samples were found to be homogeneous in L/P ratio as determined by sucrose density gradient. Aliquots were taken to determine the protein (Markwell et al., 1981) and phosphatidylcholine content (Rouser et al., 1970) to give the L/P ratios of the samples. Thin-layer chromatography revealed no evidence for lipid decomposition after NMR measurements.

NMR Measurements. NMR spectra were recorded on a home-built 360-MHz (H_0 = 8.4 T) spectrometer equipped with a Nicolet pulse programmer at 55.3 MHz (^{2}H nucleus) and 145.7 MHz (^{31}P nucleus). Deuterium spin–lattice relaxation times (T_{1z}) were measured by a standard inversion–recovery experiment ($180°_x$–τ–$90°_x$–acquisition pulse sequence). The deuterium spin–spin relaxation times (T_{2e}) were measured at 46.1 MHz on a Bruker CXP-300 spectrometer (H_0 = 7.0 T) with quadrupole-echo pulse sequences ($90°_x$–τ–$90°_y$–τ–acquisition). The quadrupole echo experiments were performed on-resonance, and all signal intensity was phased in the real channel. T_{1z} and T_{2e} were determined by a least-squares fit of the spectral intensities and spin-echo amplitude, respectively. ^{31}P NMR spectra were recorded without broad-band proton decoupling. The NMR spectrometers were equipped with a nitrogen gas flow variable-temperature unit. The temperature was measured to an accuracy of ±0.5 deg.

The instrumental parameters for ^{2}H NMR measurements were (H_0 = 8.4 T) spectral width = 20000 Hz, time domain = 1K, size = 4K, initial delay = 25 μs, number of scans = 1000, pulse width = 12 μs (90° pulse), and relaxation delay = 250 ms.

The instrumental parameters for T_{2e} experiments were (H_0 = 7.0 T) spectral width = 250000 Hz, time domain = 4K, size = 4K, pulse width = 5 μs (90° pulse), relaxation delay = 250 ms, and dwell time = 2 μs.

For phosphorus-31 NMR measurements, the instrumental settings were spectral width = 20000 Hz, time domain = 1K, size = 4K, initial delay = 25 μs, number of scans = 10000, pulse width = 16 μs (90° pulse), relaxation delay = 8 s, and no broad-band proton decoupling.

Electron Microscopy. The samples were frozen rapidly (10^5 K s^{-1}) according to the sandwich technique with liquid propane (Sternberg et al., 1989) from temperatures well above the gel to liquid-crystalline phase transition temperatures of DMPC, 23.5 °C. The samples were fractured and shadowed in a Balzers BAF-400D freeze–fracture device at −150 °C. The replicas were examined in a Tesla BS-500 electron microscope.

Deuterium NMR Simulation of Two-Site Exchange. Motional effects in deuterium NMR spectra can be treated by addition of the rate equations of the spin magnetization between different motional environments (Davoust & Devaux, 1982) and orientations, according to the Bloch equations. The rate equations for the transfer of spin magnetization for a two-site model are given by the exchange-coupled Bloch equations (McConnell, 1958):

$$dM_{fast}/dt = \tau_{off}^{-1}M_{slow} - \tau_{on}^{-1}M_{fast} \quad (1a)$$

$$dM_{slow}/dt = -\tau_{off}^{-1}M_{slow} + \tau_{on}^{-1}M_{fast} \quad (1b)$$

where M_{fast} is the spin magnetization for fluid lipids and a certain fraction of the solvation lipids at the protein interface which are in fast exchange with the fluid lipid pool and M_{slow} is the spin magnetization for another fraction of lipids associated with the protein which exchange slowly with the other lipid pools. The probabilities per unit time of transfer of lipids between these two environments are τ_{off}^{-1} and τ_{on}^{-1}. The equations assume rapid mixing of the lipids within each lipid pool by lateral diffusion. At exchange equilibrium, $dM_{fast} = dM_{slow} = 0$, and hence, the ratio of the transfer rates is related to the steady-state populations of the two lipid environments:

$$\tau_{off}^{-1}/\tau_{on}^{-1} = f/(1-f) \quad (2)$$

where $1-f$ is the fraction of lipids at the protein interface in slow exchange with the fluid lipid pool.

The steady-state exchange-coupled Bloch equations can be given in terms of complex magnetizations as

$$[\Gamma_{fast} + \tau_{on}^{-1} - i(\omega - \omega_{fast})]M_{fast} - \tau_{off}^{-1}M_{slow} = i\gamma B_i M_0 f \quad (3a)$$

$$[\Gamma_{slow} + \tau_{off}^{-1} - i(\omega - \omega_{slow})]M_{slow} - \tau_{on}^{-1}M_{fast} = i\gamma B_i M_0(1-f) \quad (3b)$$

where the line-width parameters Γ_{fast} and Γ_{slow} are derived from the respective transverse relaxation times and an allowance was made for inhomogeneous line broadening [$\Gamma = 1/(\pi T_{2e}) + \Gamma_0$]. The terms ω_{fast} and ω_{slow} are the angular resonance frequencies for the fluid pool and protein-associated deuterated lipids in slow exchange with the fluid lipid pool, respectively. M_0 is the total spin magnetization of the system ($M_{fast} + M_{slow}$), B_i is the magnetic field strength, and γ is the gyromagnetic ratio. The imaginary part of the total spin magnetization gives the line shape as the NMR spectrum is collected about ω.

Strictly speaking, the above equations give the steady-state line shapes in the frequency domain. The imaginary part of the total spin magnetization yields a line-shape formula, and line-broadening effects can provide a way to estimate the transfer rate. A complete description of the pulse experiments including the effects of pulse delay times (2τ) requires the solution of the time-dependent Bloch equations (Woessner, 1961). This method is particularly powerful as the exchange rate becomes comparable with the frequency separation of the

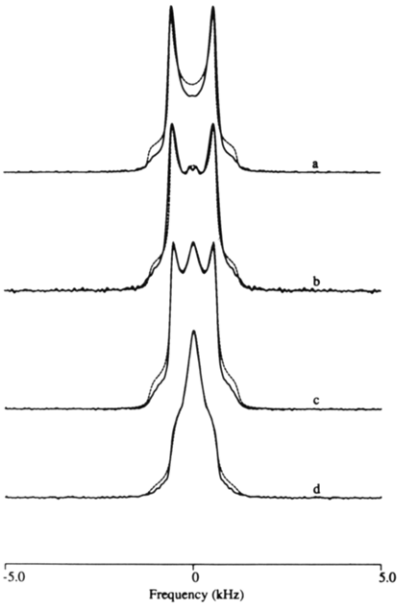

FIGURE 1: Quadrupole echo deuterium NMR spectra of DMPC-d_9/M13 coat protein complexes (—) and simulations (---) at 35 °C: (a) pure lipid; (b) L/P = 40:1 (mol/mol); (c) L/P = 25:1; (d) L/P = 12:1.

two motionally distinct environments.

To simulate the entire line shape for an anisotropic spectrum, a summation must be made over all angular orientations θ of the deuterium director axis relative to the magnetic field (B_i). In the slow-exchange regime, both the correlated and the uncorrelated jump models for reorientation of the director axis during the exchange event yield very similar spectra (Davoust & Devaux, 1982), whereas in the fast-exchange limit the uncorrelated jump model yields quasi-isotropic spectra and the correlated jump model gives anisotropic line shapes. In the NMR line-shape simulations the uncorrelated jump model is most appropriate, and each Lorentzian line shape, $L_{\text{fast}}(\theta_i)$, in the fast-exchanging component is exchanged with a sum of weighted Lorentzians, $\sum_j \rho(\theta_j) L_{\text{fast}}(\theta_j)$, in the slow-exchange component, the weighing factor being $\rho(\theta) = \sin\theta\, d\theta$. Simulations over an isotropic distribution of θ_i will therefore give the experimentally observed line shape.

For simulations of deuterium NMR spherically averaged powder patterns, the parameters needed are the deuterium quadrupolar splitting $\Delta\nu_q$ and the line-width parameter for both spectral components (assuming axial symmetry). In addition, the contributions to the two-component spectrum of each spectral component, f and $1 - f$, and the exchange frequency, τ_{ex}^{-1}, are required, where

$$\tau_{ex}^{-1} = \tau_{off}^{-1}(1 - f) = \tau_{on}^{-1} f \qquad (4)$$

The best fit of the multiparameter optimalization was obtained in two stages. First, the deuterium NMR spectrum for labeled phospholipids in protein-free bilayers was fitted to a single-component simulated line shape in order to determine $\Delta\nu_{q,\text{fast}}$ and the best matching line-width parameter, Γ_{fast}. For the protein-associated spectral component an isotropic quadrupole splitting (0 Hz) and a line-width parameter, derived by extrapolation of the T_{2e} relaxation times in the lipid/protein titration, were used. The line-width parameters, Γ, are required to match the experimentally determined spin–spin relaxation times. In the second stage of the simulation, only the population factor of both lipid environments and the exchange rate was optimized, which was achieved by quadratic minimization of the error function.

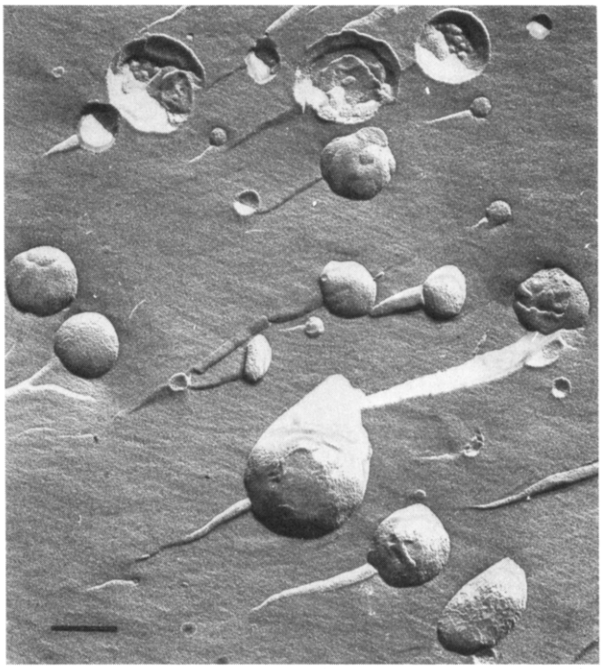

FIGURE 2: Freeze–fracture electron micrograph of DMPC/M13 coat protein complex with L/P ratio of 12:1; bar represents 500 nm. Over 95% of the lipid has been incorporated in vesicles with diameters ranging from 400 nm to 1.0 μm.

Results

Deuterium NMR Spectra. Deuterium NMR spectra of DMPC-d_9/M13 coat protein complexes with L/P ratios of 12:1, 25:1, and 40:1 and protein-free bilayers are shown in Figure 1. All the spectra were recorded at 35 °C, well above the gel to liquid-crystalline phase transition temperature, so motionally averaged, axially symmetric spectra of narrow quadrupolar splittings were observed (Figure 1a). Introducing M13 coat protein to the lipid system gives rise to a second, well-defined isotropic ^{2}H NMR spectral component. The isotropic ^{2}H NMR spectral component increases with increasing protein concentration and is very similar in shape at all protein concentrations. Thus the isotropic, second spectral component is assumed to arise from labeled DMPC molecules interacting with the M13 coat protein. The spectrum from the protein-associated lipid showed no well-resolved quadrupole splitting, which is conventionally determined from the 90° orientation contribution to the spherically averaged powder pattern as shown in the upper spectrum in Figure 1 (Seelig & Seelig, 1980). This indicates that the deuterated choline methyl groups may be disordered or have an altered conformation in the presence of M13 coat protein.

The collapse of spectral anisotropy for protein-associated lipids is not caused by motional averaging due to vesicle rotation, since the vesicles produced have large diameters ranging from 0.4 to 1.0 μm (L/P = 12:1, Figure 2) and rotate too slowly in the highly viscous samples to average the deuterium quadrupole splittings (Stockton et al., 1976; Burnell et al., 1980). In addition, the protein is mixed uniformly throughout individual bilayers, since the protein/lipid complexes are homogeneous as determined by sucrose density gradient centrifugation.

Some spectral changes in the spherically averaged powder patterns were observed on addition of the protein to DMPC-d_9 bilayers (Figure 1). The quadrupole splitting of the axially symmetric powder pattern decreases from 1180 to 1120 Hz (Figure 1a–c) on addition of up to 25:1 mol/mol M13 coat protein to DMPC vesicles; any further change at higher protein

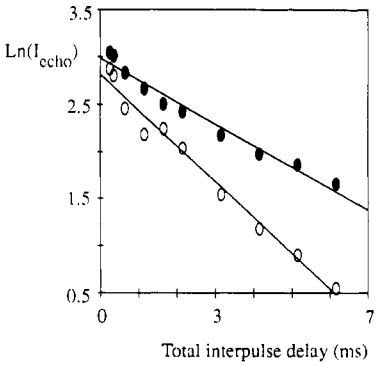

FIGURE 3: Decay of the spin-echo intensity with interpulse delay times (2τ) for pure lipid vesicles (○) and complexes with 5:1 mol/mol M13 coat protein (●). The spin-echo decays are fitted to a single exponential to determine the spin–spin relaxation times.

concentration is difficult to quantitate because of the overlapping central isotropic component. The effective line widths of both components increase with increasing protein content. The half-width of the axially symmetric spectrum was 88 Hz in the case of DMPC vesicles, which increased to ~200 Hz in the presence of 25:1 mol/mol M13 coat protein (Figure 1c). The central isotropic component displays a non-Lorentzian line shape, and so its half-width cannot be measured directly even at the highest protein content (Figure 1d). Essentially similar spectral changes were observed at higher temperatures in the range 35–50 °C (spectra not shown).

Spin–Lattice Relaxation Times. Spin–lattice (T_{1z}) relaxation time measurements give information about the fast local motions ($\tau_c \sim 10^{-10}$ s) of the deuterated segment of the phospholipid headgroup in bilayers. In protein-free bilayers of DMPC-d_9, the T_{1z} relaxation time increases from 44 ms at 30 °C to 76 ms at 50 °C. The increase in T_{1z} relaxation time with temperature indicates that the local motions are in the fast correlation time limit (Abragam, 1961). The activation energy for the rotation of the CD_3 groups of the choline headgroup about their symmetry axis was measured to be 23 kJ mol^{-1} from 30 to 50 °C. The T_{1z} relaxation time of the central component, determined on the samples with high protein concentration (L/P = 12:1 and 5:1), is rather similar to that of the pure lipid system. The T_{1z} relaxation time increases from 50 ms at 30 °C to 78 ms at 50 °C, giving an activation energy of the methyl group rotation in the presence of M13 coat protein of 20 kJ mol^{-1} over this temperature range, this being approximately 20% lower than that for protein-free bilayers. The M13 coat protein does, therefore, not significantly reduce the rapid molecular motions of the bilayer surface, which is in agreement with the earlier results on other lipid/protein systems [for a review, see Bloom and Smith (1985)].

Spin–Spin Relaxation Times. The decay of the quadrupole echo (T_{2e}) rather sensitively reflects any slow motional modulation due to lipid/protein interactions. Typical decay curves for pure DMPC vesicles and a DMPC/M13 coat protein complex of 5:1 mol/mol are shown in Figure 3, and the transverse relaxation times of protein/lipid complexes with various L/P ratios are shown in Table I. Clearly, the single-exponential decay of pure DMPC vesicles (T_{2e} = 2.7 ms) becomes more complex in the presence of the protein, although no separate components corresponding to fluid and protein-associated lipids could be resolved due to the spectral effects of intermediate exchange (for discussion, see below). With increasing protein content the effective decay time, determined by a single-exponential curve fit, increased linearly, and the approximate value of the protein-associated lipids was estimated by extrapolation using the lipid/protein titration to be $T_{2e} \sim 9$ ms (L/P = 0 mol/mol).

Table I: Spin–Spin Relaxation Times, Proportion of Isotropic Component, and Exchange Rate of Lipids between the Trapped Site and the Fluid Lipid Pool of DMPC-d_9/M13 Coat Protein Complexes with Varying L/P Ratios at 35 °C[a]

L/P ratio	T_{2e} (ms)	τ_{ex}^{-1} (Hz)	$1-f$	τ_{off}^{-1} (Hz)
5:1	6.10	125	0.51	245
12:1	4.20	70	0.33	215
25:1	2.90	25	0.11	235
40:1	2.75	15	0.07	215
protein free	2.70			

[a] The estimated errors are 0.2 ms (T_{2e}), 0.02 ($1-f$), and 50 Hz (τ_{off}^{-1}).

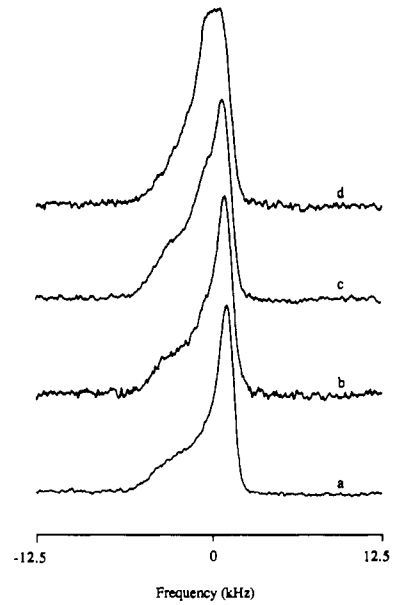

FIGURE 4: Phosphorus-31 spectra of DMPC-d_9/M13 coat protein complexes at 30 °C: (a) pure lipid; (b) L/P = 40:1 (mol/mol); (c) L/P = 25:1; (d) L/P = 12:1. No proton decoupling.

Phosphorus-31 NMR. Phosphorus-31 NMR experiments on the DMPC-d_9/M13 coat protein complexes indicate that the lipids are arranged in bilayers (De Kruijff et al., 1985). The phosphorus-31 spectra for DMPC/M13 coat protein complexes with L/P ratios of 12:1, 25:1, and 40:1 and for pure DMPC bilayers at 30 °C are shown in Figure 4. Phosphorus-31 NMR spectra of protein-free bilayers of DMPC show a CSA of −45 ppm. In the presence of M13 coat protein, a second spectral component is observed, which is well displayed in the complex with a L/P ratio of 12:1. The intensity of the second phosphorus-31 NMR spectral component increases with protein concentration and has a CSA value of less than −20 ppm, but was not quantitated.

^2H NMR Spectral Simulations. The decreasing quadrupole splitting and the accompanying line-broadening effects in DMPC/M13 coat protein complexes can be accounted for only by two-site chemical exchange between the fluid and protein-associated lipid phases with different quadrupole splittings. Following Kang et al. (1979) an estimate can be given for the exchange rate from the decrease in the quadrupole splitting, and $\tau_{ex}^{-1} \sim 10^2$ Hz is obtained. This rate corresponds to slow exchange on the deuterium NMR time scale and is, hence, expected to produce partial averaging of the two components in agreement with the spectral effects seen in Figure 1. Slow exchange can also explain the apparent counter behavior between the observed line broadening and the increasing spin–spin relaxation times.

In the spectral simulations a central isotropic component was attributed to the protein-associated lipids; Oldfield and his co-workers made the same assumption on the basis of the NMR spectra recorded in the L_β phase in the DMPC/cytochrome *c* oxidase system (Kang et al., 1979). The line width of this component was estimated by extrapolating the T_{2e} values to L/P = 0, and an effective half-width of 30 Hz was obtained; no spread in quadrupole splitting was assumed. The axially symmetric powder pattern of $\Delta\nu_q$ = 1173 Hz was essentially the same as that observed for pure DMPC, and so its approximate line width was determined from the T_{2e} experiments, and a half-width of 88 Hz was used in subsequent simulations. The less satisfactory fit at the 0° edges (Figure 1) can be explained by magnetic orientation effects (Seelig et al., 1985), anisotropic T_{2e} relaxation (Sternin, 1982), or instrumental factors. The relative contributions of these two mechanisms can only be estimated from a series of partially relaxed spectra (Meier et al., 1986, 1987) since it is only this latter mechanism that leads to a progressive "pseudo-dePaking". However, the fitting error, defined as the squared deviation between the experimental and simulated spectra, was only slightly affected by these additional terms in the line-shape formula, and therefore no attempt was made to reduce the apparent mismatch because it would have introduced further line-shape parameters into the fitting program.

Two-component exchange-averaged line shapes were calculated by solving the steady-state modified Bloch equations; motional effects other than those due to exchange were not treated explicitly and were represented by an effective line-width (isotropic) parameter. With the above spectral components, two further parameters need to be adjusted to obtain a good fit: the relative intensity factors of the two components, f, and the exchange rate between the two motionally distinct environments, τ_{ex}^{-1}. A linear (nonexchanging, τ_{ex}^{-1} = 0 Hz) combination of these two Lorentzian line shapes gave rather poor fits to the experimental spectra, and even a gradually increasing line width for the protein-associated component brought obviously no significant improvements. The best-fitting line shapes shown in Figure 1 superimposed upon the respective experimental NMR spectra are all in good agreement for the various L/P ratios and were calculated by assuming an intermediate exchange of τ_{ex}^{-1} = 15–125 Hz. As expected from the detailed balance of one-to-one exchange (cf. eq 4), the off-rates were independent of the L/P ratio; τ_{off}^{-1} = 230 ± 50 Hz (Table I).

After exchange had been compensated for through spectral simulations, the fraction of the isotropic spectral component $(1 - f)$ was quantified and found to increase with decreasing L/P ratio (Table I). From the linear quantitation of the ratio of both spectral components, $f/(1 - f)$, with the L/P molar ratio, an estimate of the number of protein-associated lipids per protein monomer was made to give a value of 3–3.5 for the number of binding sites of lipids per protein in slow exchange with the fluid lipid pool (Brotherus et al., 1981). All these fractions and the extrapolated number of binding sites were lower by ~25% than the corresponding values of 4 reported for the same system by spin-label ESR spectroscopy (Wolfs et al., 1989).

Discussion

Previous ESR experiments on DMPC/M13 coat protein complexes (Wolfs et al., 1989) have been performed to demonstrate lipid/protein interactions of the lipid molecule in the acyl chains with the protein. In the present study, interactions of M13 coat protein with the lipid headgroup are investigated with the aim of obtaining information on the lipid/protein interactions. In addition, if any molecular specificity occurs in the interaction, this is most probably where it would manifest itself (Watts, 1987, 1989).

Two-component deuterium NMR spectra were obtained for DMPC-d_9/M13 coat protein complexes. Since the vesicles formed were homogeneous in L/P ratio and had diameters of 0.4–1.0 μm (L/P = 12:1), the intensity of the central component is suggested to arise from protein-associated lipid. Furthermore, the isotropic spectrum cannot be ascribed to residual HDO because it has relaxation times similar to those of lipids (rather than to HDO) in protein-free bilayers of DMPC. The collapse in the spherically averaged powder ^{2}H NMR spectra suggests that the terminal methyl groups are disordered or have an altered conformation in the presence of M13 coat protein when compared with protein-free bilayers. In DMPC-d_9/M13 coat protein complexes, the exchange rate between bulk lipid and lipid at the protein interface is slower than 1.0 kHz. Further evidence in support of slow exchange was obtained by phosphorus-31 NMR of DMPC-d_9/M13 coat protein complexes, which also showed two-component NMR spectra (Figure 4). The exchange rate (τ_{ex}^{-1}) of lipids between the M13 coat protein complexes and the protein-free bilayer is therefore slower than the difference in CSA of phospholipids in the two environments, which would be ~3.6 kHz (25 ppm) to give rise to two-component phosphorus-31 NMR spectra from a single, homogeneous complex.

More detailed information about the molecular exchange was obtained by spectral simulations of the deuterium NMR spectra shown in Figure 1. An off-rate for the lipid from the protein-associated environment of τ_{off}^{-1} = 0.23 kHz was estimated from the simulation at all L/P ratios studied. This exchange rate is much slower than the off-rate of 14-PCSL in DMPC/M13 coat protein complexes determined by ESR spectroscopy (τ_{off}^{-1} ~ 5.0 MHz) (Wolfs et al., 1989). The apparent discrepancy in the lipid exchange rates as determined by the two spectroscoipic techniques may be explained by considering three possible motional environments for the lipids in the protein-containing complexes. M13 coat protein has a predominantly β-sheet structure, thus giving the protein a tendency to aggregate very strongly (Datema et al., 1988b). One possible packing arrangement for aggregation which would maintain a constant number of lipid solvation sites per protein molecule (Figure 5) is for the M13 coat protein to aggregate in one dimension only ("linear aggregates"). Lipid molecules can now be situated in one of three environments: (i) between the closely packed parallel aggregates ("trapped lipid"); (ii) at the outside of the lipid/protein complex ("boundary lipid"); (iii) in the bulk phase ("bulk lipid"). The first two lipid environments are closely associated with the protein but have different exchange rates with the bulk lipid. The lipids situated between closely packed parallel protein aggregates are trapped and therefore exchange rather slowly to the fluid lipid pool (τ_{off}^{-1} = 0.23 kHz from present simulations). On the other hand, lipids situated at the boundary of the lipid/protein aggregate exchange more rapidly to the fluid lipid pool (τ_{off}^{-1} ~ MHz). In spin-label ESR spectroscopy, anisotropy averaging of the electron–nitrogen-14 hyperfine interactions is sensitive to motions on the order of $\tau_c \sim 10^{-9}$–10^{-8} s. Thus, both types of the protein-associated lipid (trapped and boundary) will give rise to a similar ESR spectral component, indicative of restricted motion of the spin-label without discrimination between either type of motional restriction. However, in deuterium NMR spectroscopy, the quadrupole splitting anisotropy averaging is sensitive to much slower motions, $\tau_c \sim 10^{-3}$ s, and only trapped

lipid molecules with exchange rates (τ_{ex}^{-1} < kHz) will contribute to the central spectral component. The boundary lipid molecules exchange too rapidly with the bulk lipid on the deuterium NMR time scale to contribute to the central spectral component and consequently will give rise to an averaged bulk lipid spectrum, with possibly a slightly decreased quadrupole splitting in comparison with protein free bilayers, as observed in other systems (Watts, 1987). Therefore, the x-axis intercept of 3–3.5 lipids per protein monomer [$f/(1-f)$ vs L/P ratio] represents the average number of trapped lipids per protein molecule rather than the total (trapped and boundary) number of 4 lipids associated per M13 coat protein monomer as determined by ESR spectroscopy (Wolfs et al., 1989). The y-axis intercept, reflecting the average binding constant, is −1 because the probe and host lipid are the same lipid molecules (Brotherus et al., 1981). In this discussion, no assumptions are made about how many M13 monomers are associated to form a protein unit capable of aggregating linearly, nor is it clear whether the aggregates are straight or simple parallel aggregates.

Two-component deuterium NMR spectra were also observed in the case of DMPC/M13 coat protein complexes, probed with chain-deuterated palmitic acid (Datema et al., 1988a). The trapped palmitic acid may have contributed to the isotropic central component. The quadrupole splittings for these labeled lipids were much larger, and therefore, the line broadening due to chemical exchange would have been small. It should be noted that such slowly exchanging protein-associated lipid phases are not present in every lipid/protein system studied so far and that the aggregated M13 coat protein may represent rather an exception than a rule.

Elongated structures of fd coat protein in aqueous solution have been observed by electron microscopy (Cavalieri et al., 1976). Also, the cardiolipin synthesis by an M13-infected *E. coli* cell is increased (Chamberlain et al., 1976), and it is possible that M13 coat protein selectively decreases the cardiolipin content of the cell membrane by trapping it between the M13 coat protein aggregates during storage. The high affinity of M13 coat protein for cardiolipin has been demonstrated in earlier ESR studies (Datema et al., 1987b). The high local protein concentration in lipid bilayers and the linear format of the M13 protein aggregates may be important for the rapid assembly of phage particles before bacteriophage extrusion.

Acknowledgments

We thank the Oxford Enzyme Group for the use of the Nicolet-360 NMR spectrometer and T. W. Poile, M. Sami, and J. C. Sanders for useful discussions.

Registry No. DMPC, 18194-24-6.

References

Abragam, A. (1961) *The Principles of Nuclear Magnetism*, Oxford University Press, Oxford.

Beck, E., Sommer, R., Auerwald, E., Kurz, C., Zink, B., Oosterburg, G., Schaller, M., Sugimoto, K., Sugisaki, H., Okamoto, T., & Takamani, M. (1978) *Nucleic Acids Res. 5*, 4495–4503.

Bloom, M., & Smith, I. C. P. (1985) in *Progress in Protein-Lipid Interactions* (Watts, A., & De Pont, J. J. H. H. M., Eds.) Vol. 1, pp 61–88, Elsevier Science Publishers, Amsterdam.

Bogusky, M. J., Schiksius, R. A., & Opella, S. J. (1987) *J. Magn. Reson. 72*, 186–190.

Brotherus, J. R., Griffith, D. H., Brotherus, M. D., Jost, J. R., & Hokin, L. E. (1981) *Biochemistry 20*, 5261–5267.

Burnell, E. E., Cullis, P. R., & de Kruijff, B. (1980) *Biochim. Biophys. Acta 603*, 63–69.

Cavelieri, S., Goldthwait, D., & Neet, K. (1976) *J. Mol. Biol. 102*, 713–722.

Chamberlain, B. K., & Webster, R. E. (1976) *J. Biol. Chem. 24*, 7739–7745.

Chamberlain, B. K., Nozaki, Y., Tanford, C., & Webster, R. E. (1978) *Biochim. Biophys. Acta 510*, 18–37.

Cross, T. A., & Opella, S. J. (1980) *Biochem. Biophys. Res. Commun. 92*, 478–484.

Datema, K. P., Visser, A. J. W. G., Van Hoek, A., Wolfs, C. J. A. M., Spruijt, R. B., & Hemminga, M. A. (1987a) *Biochemistry 26*, 6145–6152.

Datema, K. P., Wolfs, C. J. A. M., Marsh, D., Watts, A., & Hemminga, M. A. (1987b) *Biochemistry 26*, 7571–7574.

Datema, K. P., Spruijt, R. B., Wolfs, C. J. A. M., & Hemminga, M. A. (1988a) *Biochim. Biophys. Acta 944*, 507–515.

Datema, K. P., Van Boxtel, B. J. H., & Hemminga, M. A. (1988b) *J. Magn. Reson. 77*, 372–376.

Davoust, J., & Devaux, P. F. (1982) *J. Magn. Reson. 48*, 475–494.

Deese, A. J., Dratz, E. A., Dahlquist, F. N., & Paddy, M. R. (1981) *Biochemistry 20*, 6420–6427.

De Kruijff, B., Cullis, P. R., Verkleij, A. J., Van Echteld, C. J. A., Taraschi, T. F., Van Hoogevest, P., Killian, J. A., Rietveld, A., & Van der Steen, A. T. M. (1985) in *Progress in Protein-Lipid Interactions* (Watts, A., & De Pont, J. J. H. H. M., Eds.) Vol. 1, pp 89–142, Elsevier Science Publishers, Amsterdam.

Eibl, H. (1980) *Proc. Natl. Acad. Sci. U.S.A. 75*, 4074–4077.

Fodor, S. P. A., Dunker, A. K., Ng, Y. C., Carsten, D., & Williams, R. W. (1981) in *Seventh Biennial Conference on Bacteriophage Assembly* (Dubow, M. S., Ed.) pp 441–445, Alan R. Liss, New York.

Garssen, G. J., Hilbers, C. W., Schoenmaker, J. G. G., & Van Boom, J. H. (1977) *Eur. J. Biochem. 81*, 453–463.

Henry, T. J., Weiner, J. H., & Sykes, B. D. (1986a) *Biochemistry 25*, 590–595.

Henry, T. J., O'Neil, J. D., Weiner, J. H., & Sykes, B. D. (1986b) *Biophys. J. 49*, 329–331.

Kang, S. Y., Gutowsky, H. S., Hshung, J. C., Jacobs, R., King, T. E., Rice, D., & Oldfield, E. (1979) *Biochemistry 18*, 3257–3267.

Knippers, R., & Hoffmann-Berling, H. (1966) *J. Mol. Biol. 21*, 281–292.

Kühn, A., Wickner, W., & Kreil, G. (1986) *Nature 322*, 335–339.

Leo, G. C., Colagno, L. A., Valentine, K. G., & Opella, S. J. (1987) *Biochemistry 26*, 854–862.

Makino, S., Woolford, J., Tanford, C., & Webster, R. (1975) *J. Biol. Chem. 250*, 4327–4332.

Markwell, M. A. K., Haas, S. M., Tolbert, N. E., & Bieber, L. L. (1981) *Methods Enzymol. 72*, 296–303.

Marvin, D. A., & Wachtel, E. J. (1975) *Nature 253*, 19–23.

Marvin, D. A., Wiseman, R. L., & Wachtel, E. J. (1974) *J. Mol. Biol. 88*, 581–598.

McConnell, H. M. (1958) *J. Chem. Phys. 28*, 430–431.

Meier, P., Ohmes, E., & Kothe, G. (1986) *J. Chem. Phys. 85*, 3598–3614.

Meier, P., Sachse, J. H., Brophy, P. J., Marsh, D., & Kothe, G. (1987) *Proc. Natl. Acad. Sci. U.S.A. 84*, 3704–3708.

Nozaki, Y., Chamberlain, B. K., Webster, R. E., & Tanford, C. (1976) *Nature 259*, 335–337.

Poile, T. W., & Watts, A. (1989) *J. Magn. Reson.* (submitted for publication).
Rouser, G., Fleisher, S., & Yamamoto, A. (1970) *Lipids 5*, 494-496.
Seelig, J., & Seeling, A. (1980) *Q. Rev. Biophys. 13*, 19-61.
Seelig, J., Borle, F., & Cross, T. A. (1985) *Biochim. Biophys. Acta 814*, 195-198.
Spruijt, R. B., Wolfs, C. J. A., & Hemminga, M. A. (1989) *Biochemistry 28*, 9158-9165.
Sternberg, B., Gale, P., & Watts, A. (1989) *Biochim. Biophys. Acta 980*, 117-126.
Stockton, G. W., Polnaszek, C. F., Tullock, A. P., Hasan, F., & Smith, I. C. P. (1976) *Biochemistry 15*, 954-966.
Van Wezenbeek, P. M. G. F., Hulsebos, T. J. M., & Schoenmakers, J. G. G. (1980) *Gene 11*, 129-148.
Watts, A. (1987) *J. Bioenerg. Biomembr. 19*, 625-653.
Watts, A. (1989) *Curr. Opinions Cell Biol. 1*, 691-700.
Wickner, W. (1976) *Proc. Natl. Acad. Sci. U.S.A. 73*, 1159-1163.
Woessner, D. (1961) *J. Chem. Phys. 35*, 41-48.
Wolfs, C. J. A. M., Horváth, L. I., Marsh, D., Watts, A., & Hemminga, M. A. (1989) *Biochemistry 28*, 9995-10001.

Photosynthetic Reaction Center of Green Sulfur Bacteria Studied by EPR†

Wolfgang Nitschke,*,‡ Ute Feiler,§ and A. William Rutherford‡

Service de Biophysique, Dêpartement de Biologie, CEN Saclay, 91 191 Gif sur Yvette Cedex, France, and Max-Planck-Institut für Biophysik, Heinrich Hoffmann Strasse 7, 6000 Frankfurt am Main 71, FRG

Received October 9, 1989; Revised Manuscript Received December 20, 1989

ABSTRACT: Membrane preparations of two species of the green sulfur bacteria *Chlorobium* have been studied by EPR. Three signals were detected which were attributed to iron–sulfur centers acting as electron acceptors in the photosynthetic reaction center. (1) A signal from a center designated F_B, (g_z = 2.07, g_y = 1.91, g_x = 1.86) was photoinduced at 4 K. (2) A similar signal, F_A (g_z = 2.05, g_y = 1.94, g_x = 1.88), was photoinduced in addition to the F_B signal upon a short period of illumination at 200 K. (3) Further illumination at 200 K resulted in the appearance of a broad feature at g = 1.78. This is attributed to the g_x component of an iron–sulfur center designated F_X. The designations of these signals as F_B, F_A, and F_X are based on their spectroscopic similarities to signals in photosystem I (PS I). The orientation dependence of these EPR signals in ordered *Chlorobium* membrane multilayers is remarkably similar to that of their PS I homologues. A magnetic interaction between the reduced forms of F_B and F_A occurs, which is also very similar to that seen in PS I. However, in contrast to the situation in PS I, F_A and F_B *cannot* be chemically reduced by sodium dithionite at pH 11. This indicates redox potentials for F_A and F_B which are lower by at least 150 mV than their PS I counterparts. The triplet state of P_{840}, the primary electron donor, could be photoinduced at 4 K in samples which had been preincubated with sodium dithionite and methyl viologen and then preilluminated at 200 K. The preillumination reduces the iron–sulfur centers while the preincubation is thought to result in the inactivation of an earlier electron acceptor, possibly the double reduction of a quinone which could occur at potentials higher than those associated with its functional one-electron couple. Orientation studies of the triplet signal in ordered multilayers indicate that the bacteriochlorophylls which act as the primary electron donor in *Chlorobium* are arranged with a structural geometry almost identical with that of the special pair in purple bacteria. The *Chlorobium* reaction center appears to be similar in some respects to both PS I and to the purple bacterial reaction center. This is discussed with regard to the evolution of the different types of reaction centers from a common ancestor. This has significance to the current understanding of the structure of the PS I reaction center.

Green photosynthetic bacteria (Chlorobiaceae and Chloroflexaceae) are morphologically quite distinct from other photosynthetic bacteria. They contain mainly bacteriochlorophyll (BChl)[1] *a* and *c* and have a unique antenna system called the chlorosome. Recent work, however, has demonstrated that this morphological classification is somewhat misleading. On the basis of 16 S-RNA sequences, it can be concluded that the green *non*-sulfur bacteria (Chloroflexaceae) are actually not very closely related to the green sulfur bacteria (Chlorobiaceae) (Woese, 1987).

The reaction center of *Chloroflexus aurantiacus* has been shown to possess pronounced similarities to the photosynthetic reaction center of purple bacteria (Shuvalov et al., 1986; Shiozawa et al., 1987; Blankenship et al., 1988; Ovchinnikov et al., 1988a,b). The structure of the purple bacterial reaction center which has been determined by X-ray crystallography

†W.N. was supported by the Deutsche Forschungsgemeinschaft (DFG), U.F. was supported by the Leibnitz-Programm (to H. Michel) of the DFG and by the Max-Planck-Gesellschaft, and A.W.R. was supported by the CNRS (URA 1290).
‡CEN Saclay.
§Max-Planck-Institut für Biophysik.

[1] Abbreviations: RC, reaction center complex; BChl, bacteriochlorophyll; FeS center, iron–sulfur center; P_{840}, primary electron donor bacteriochlorophyll(s) of green sulfur bacteria; P_{700}, primary electron donor chlorophyll(s) of PS I; PS I, photosystem I; ZFS, zero-field splitting parameters of the spin-polarized spectrum of the triplet state of the primary donor.

0006-2960/90/0429-3834$02.50/0